JOURNAL OF GEOPHYSICAL RESEARCH, VOL. 98, NO. D6, PAGES 10,375–10,384, JUNE 20, 1993

Correlations of Atmospheric Dynamics With Solar Activity Evidence for a Connection via the Solar Wind, Atmospheric Electricity, and Cloud Microphysics

BRIAN A. TINSLEY AND RODERICK A. HEELIS

Center for Space Science, University of Texas at Dallas

We respond to several criticisms of the view that there is a physical linkage between solar activity and the dynamics of the troposphere and lower stratosphere, and we provide further evidence in support of a mechanism for such a linkage involving atmospheric electricity and cloud microphysics. The main criticisms are (1) that the decadal time scale variations in stratified data result from aliasing introduced by the sampling process and are not responses to a decadal time scale physical input; (2) that the observed correlations are due to chance coincidence or an atmospheric periodicity that is not uniquely related to solar variability; and (3) that there are no plausible mechanisms that can amplify one of the weak solar-varying inputs in the region where the correlations are found. We show that the aliasing criticism is inadequate because the real quasi-biennial oscillation departs from an ideal sine wave in a way that reduces aliasing effects to insignificant levels. The nonuniquenessof identification of the 11-year solar cycle as the period of the arctic forcing for the Arctic winter stratospheric temperatures is a problem only for the short 33-year record of polar temperatures; in much longer time series of unstratified climate data the periods of 11 and 22 years are prominent. Highly unique signatures of solar wind forcing of tropospheric dynamics exist on the day-to-day time scale via two independent inputs to atmospheric electricity. These are (1) through changes in tropospheric ion production as a result of solar wind modulation of galactic cosmic rays and (2) through changes in the potential difference between the polar ionospheres and the surface, forced by the solar wind By component. The product of the cosmic ray flux and the ionospheric potential determines the vertical air-earth electrical current. In the presence of clouds of large horizontal extent, this current determines the rate of polarization charging of the clouds via the accumulation of positive electrostatic charges on droplets near cloud tops. The observed correlations, and theoretical and laboratory results for the effects of electrostatic charges on droplets and aerosols on the rates of ice nucleation, are consistent with the postulate that for certain regions and seasons and atmospheric levels the large-scale atmospheric electrical parameters have significant effects on the rates of initial ice nucleation. In such cases the chain of consequences includes changes in the rates of precipitation, net latent heat release, vertical motions, atmospheric vorticity, and ultimately in the general circulation. Much more work is required before the mechanism can be considered to have a secure basis in laboratory experiment and quantitative atmospheric modeling.

1. INTRODUCTION

There have been many reports of apparent responses of the lower atmosphere dynamics and temperature and precipitation to variations in solar activity. One of the more striking correlations has been found between the winter stratospheric temperature in the Arctic and the 11-year sunspot cycle [*Labitzke*, 1987; *Labitzke and van Loon*, 1988]. This was obtained by stratifying data for individual winters according to whether the direction of stratospheric winds at 45 mbar in the equatorial regions was from the west (west phase) or from the east (east phase). These winds oscillate with an approximate 28-month period; therefore the phenomenon is called the quasi-biennial oscillation (QBO) of equatorial stratospheric winds. Figure 1 is an update of these results; it shows that the correlation has persisted for the years subsequent to 1986. For the west phase, the temperature excursion between about -75° and -60° C shows a strong positive correlation with the 10.7-cm solar flux, representing the solar cycle, whereas for the east phase the temperature excursion over the same range shows a moderately strong anticorrelation. For unstratified data the correlation is much weaker. We will analyze in Section 2 the argument that these and, by implication, similar results for tropospheric dynamics and atmospheric ozone and electric field changes represent an aliasing effect introduced by the sampling process and are not responses to a decadal time scale physical input.

The observations of winter stratospheric temperatures correlated with the solar cycle extend over only 33 years, which is not long enough to uniquely identify the 11-year sunspot cycle as the period of the forcing. We will show in Section 3 that in much longer time series of atmospheric data, the solar (and solar wind magnetic structure) periods of 11 and 22 years are prominent.

The lack of a mechanism that can amplify a weak solar input in the region where the correlations are found has been stated in essentially all critical discussions as a weakness of the view that correlations between atmospheric parameters and solar variability are caused by real physical connections. What calls for explanation is not only the *Labitzke and van Loon* [1988] results for decadal oscillations in the stratosphere but also numerous reports of apparent responses to solar activity in the troposphere both on the decadal (and longer) time scales and on the day-to day time scales. The stratospheric oscillations, if real, might be excited by an in situ solar forcing, by effects propagating downward from the mesosphere and thermosphere, or by effects propagating upward from solar forcing of the troposphere. It was pointed out by *Holton* [1982] that effects are much more likely to propagate upward than downward.

For identifying processes that might link solar inputs to atmospheric responses, it is advantageous to examine short-term variations, since the several solar inputs each have unique signatures on the day-to-day time scale and it is therefore possible to identify any of the inputs that might be involved; this is not

Paper number 93JD00627.
0148-0227/93/93JD-00627$05.00

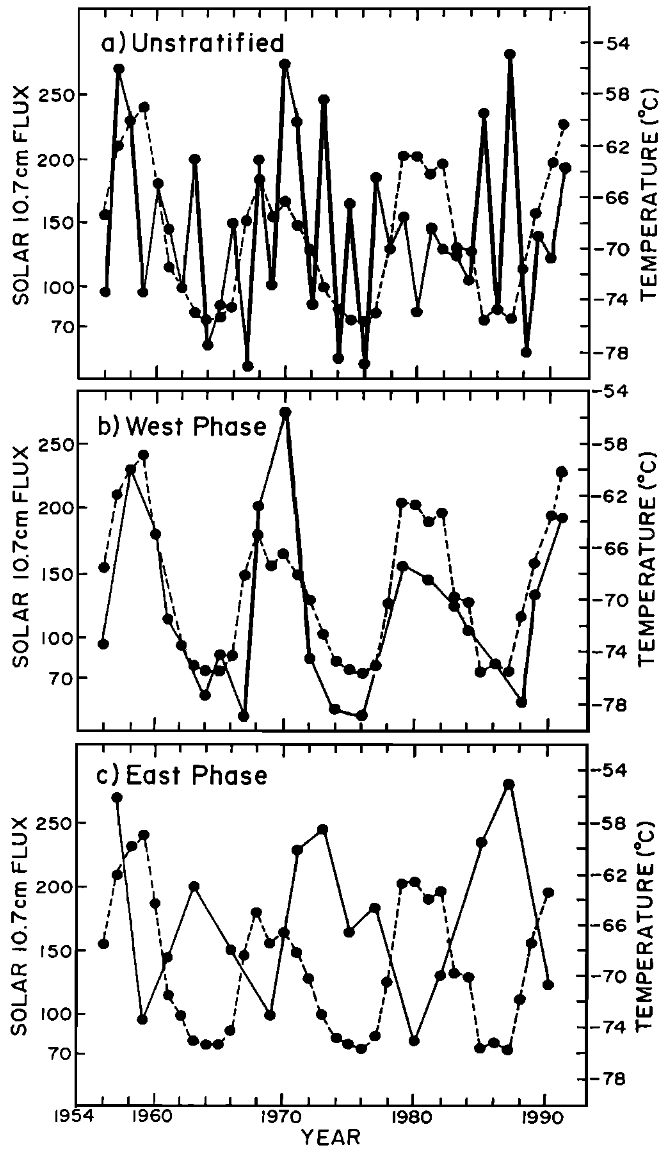

Fig. 1. Correlation between solar flux and stratospheric temperature in the Arctic from 1956 to 1989. *(a)* Unstratified data. Solid curve, January-February mean 30-mbar temperature; dashed curve, 10.7-cm solar flux. *(b)* Same as panel *a* for winters only in the west phase of the QBO. *(c)* Same as panel *a* for winters only in the east phase of the QBO.

possible on the decadal time scale. We will examine in Section 4 two independent sets of apparent responses to varying solar inputs, both of which are short term and occur in the troposphere. They point to the existence of a single physical process linking changes in tropospheric dynamics to changes in atmospheric electricity as it responds to external forcing by the solar wind. The process also implies variations in tropospheric forcing on the decadal time scale. We will discuss to what extent such tropospheric forcing, propagating upward as waves to the stratosphere while being modulated by the QBO, can account for the apparent responses there on the decadal time scale.

The possibility that the solar wind, via changes in its magnetic field, affects inputs into atmospheric electrical processes and the global electric circuit has been suggested previously [*Ney*, 1959; *Dickinson*, 1975, *Markson*, 1978]. The solar wind is the outward extension of the highly conducting solar corona, moving at supersonic speed past the earth, and it transmits to the ionosphere and global electrical circuit the effects of changes of solar activity and in the large-scale solar magnetic fields. These fields also modulate cosmic ray fluxes from galactic sources as they flow into the inner solar system. The cosmic ray flux is the dominant ionization source in the troposphere and lower stratosphere. However, the amount of energy involved in these electrical inputs into the atmosphere is a factor of about 10^9 less than the total solar irradiance and a factor of about 10^6 less than variations in the visible-infrared and UV photon inputs [*Newkirk*, 1982]. This has been an impediment to serious consideration of solar wind forcing of weather and climate. However, the solar wind-modulated electrical energy is deposited directly in the troposphere; has a relatively large amplitude as a fraction of its mean value and is an input that provides considerably more energy per particle than thermal energy for catalyzing or controlling (on the microscale) chemical and physical changes of state. This energy requires an amplification by more than a factor of 10^6 to significantly affect atmospheric dynamics. However, the mechanism proposed by *Tinsley* [1990] and *Tinsley and Deen* [1991] connecting atmospheric electricity and the rate of contact ice nucleation in clouds can satisfy that requirement on a time scale of hours. By affecting the release of latent heat, it changes vertical motions, atmospheric vorticity, and atmospheric pressure. This mechanism was proposed to explain the short-term correlations of tropospheric dynamics with short term modulation of the galactic cosmic ray flux by the solar wind during active solar conditions. We will discuss it also as a candidate to explain the completely independent correlations of tropospheric dynamics with changes in ionospheric electric fields related to changes in the solar wind magnetic fields under quiet solar conditions.

2. NATURE AND EXTENT OF ALIASING EFFECTS

The aliasing question has been emphasized by *Wallace* [1988], *Teitelbaum and Bauer* [1990], *Dewan and Shapiro* [1991], and *Salby and Shea* [1991]. The possibility is raised that the change in Arctic stratospheric temperature is due to forcing by the QBO alone (no input from the varying sun), and that the apparent correlation with the 11-year solar cycle is a result of aliasing by the annual sampling. We first test this by examining the aliasing effect of sampling a synthetic QBO and comparing the result with the observations. We then examine the aliasing effect of sampling the real QBO and comparing the results with observations. Since the temperature samples are made at 12-month intervals, for a pure sinusoid of period 28 months there would be a 2-month phase shift of each yearly datum point with respect to the synthetic QBO. With stratification of the datum points with respect to whether they were in the positive (e.g., west) or the negative (e.g., east) phase of the synthetic QBO, the result shown in Figure 2 is obtained. For both phases the stratified data show the effect of aliasing, giving a sinusoidal output of period 7 years. (When the phases are sampled separately at 12-month intervals, the sampling shifts in phase by 4 months per 28-month QBO cycle [4 = 28 - 24], so that in exactly three QBO cycles or 7 years the shifts total 12 months, repeating the initial conditions.) A key point to be noted is that for the positive phase the amplitude is the top 30% of the range of the synthetic QBO and for the negative phase it is the bottom 30%, with no overlap of the two ranges. This nonoverlap must necessarily be the case for any stratification according to positive and negative phases of the same forcing function that generates the unstratified time series. An overlap can, of course, be produced if the synthetic or real QBO is sampled with stratification by other than the synthetic or real

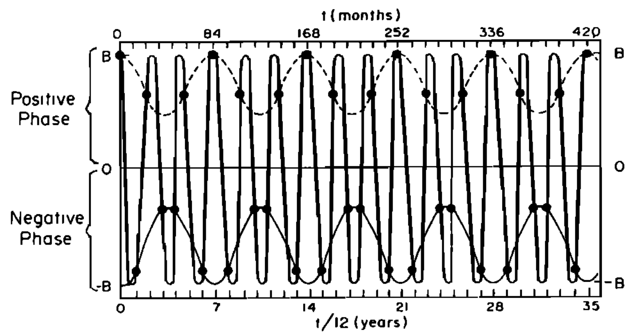

Fig. 2. Aliasing of a synthetic QBO [$A_{QBO}(t) = 1 + B\cos(2\pi t/28)$] by sampling it at 12-month intervals. Dashed curve, positive phase of the cosine term; solid curve negative phase of the cosine term.

QBO phase, as has been done in some of the studies referenced above. However, this was not the procedure used by *Labitzke and van Loon* [1988], and such stratification by other than the QBO phase does not constitute a test for the effect of aliasing in their results.

There are physical reasons for stratifying the data by the phase of the QBO, related to changes with QBO phase of stratospheric chemistry and of wave-mean flow interactions and of aerosol and electrical parameters, as will be discussed in section 5. The stratification by alternate years does not appear to have any physical basis, and certainly the stratification of samples of a synthetic QBO by the real QBO phase has no physical basis, and thus the results of such stratification are without physical significance.

Although the analysis represented by Figure 2 appears to confirm some aliasing effects, the above results have been for an unrealistic QBO. The whole discussion of the question of aliasing can be, and should be, conducted with respect to the real QBO, which is by no means a sinusoid and has by no means a constant period. Figure 3 shows plots of the actual 45-mbar equatorial stratospheric wind velocity, from observations at Canton Island, the Maldives, and Singapore (*K. Labitzke*, personal communication, 1991] for the years since 1951. Figure 3*a* is the complete time series, and the diamonds are the values of the annual sampling without stratification. Figure 3*b* is the annual sampling for the QBO west phase only, and Figure 3*c* is the same for the QBO east phase only. One can see that the sampling and stratification have produced outputs with no overlap, as expected, but surprisingly, there is very little modulation due to aliasing at the 7-year period or in the range 7-15 years. Figure 3 can be compared directly with Figure 1, and, in particular, the almost complete overlap of the variations in Figs 1*b* and 1*c* can be compared with the well-separated and small-amplitude variations in Figures 3*b* and 3*c*.

Therefore, there are two arguments against aliasing of QBO forcing (without input from the varying sun) as an explanation of the data in Figure 1. The argument just in terms of mathematics is that the sampling and stratification should produce outputs with some long period-aliasing, but no overlap of the stratified outputs. This is contrary to the observations, which show complete overlap. The second and stronger argument rests on the empirical result (as shown in Figures 3*b* and 3*c*) of sampling the real QBO, in contrast to the mathematical result of sampling a pure sinusoidal QBO, which shows even less resemblance to the observations.

As a commentary, but not as part of the argument, we note that Figure 3*a* shows the way in which the real QBO departs from a pure sinusoid: the west phase variation resembles a square wave (and the sampling of a pure square wave stratified by its own phase does not result in aliasing), and the period is variable. In the intervals from 1954 to 1964 and from 1968 to 1974, the period was shorter than average, and in the remaining intervals the period was longer. The QBO is partially phase locked to the higher-altitude semiannual oscillation [*Gray and Pyle*, 1989], tending to switch phases at about the same time each year (missing some years). A wave completely phase locked to a semiannual oscillation would show no aliasing with annual sampling.

In summary, although it is true that analyses that resemble that made by *Labitzke and van Loon* [1988] do produce seriously aliased outputs, we have shown that the actual sampling and stratification procedure used by *Labitzke and van Loon* [1988], when applied to the real QBO forcing function, produces very little aliased output with a period of 10-12 years. Therefore we conclude that aliasing of a winter Arctic stratospheric temperature change that is forced by the QBO alone is an inadequate explanation of the correlations of Figure 1. The same conclusion applies to winter circulation changes in the troposphere [*Labitzke and van Loon*, 1988; *van Loon and Labitzke*, 1988; *Venne and Dartt*, 1990; *Barnston and Livezey*, 1991; *Mason and Tyson*, 1992]; and in the middle atmosphere [*Chanin et al*, 1989]; and for winter electric field changes [*Marcz*, 1990], and to ozone changes

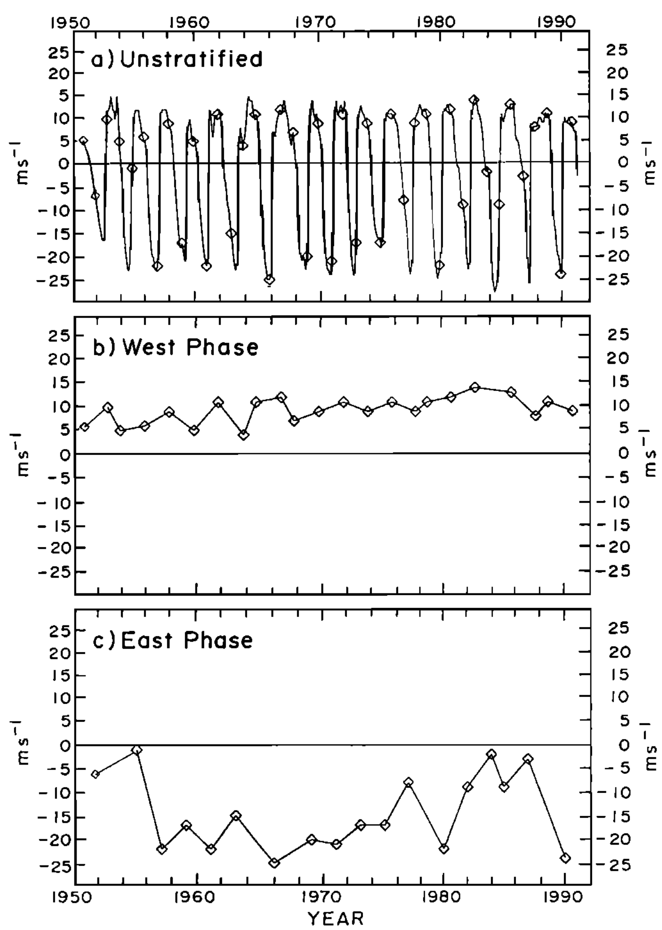

Fig. 3. Equatorial stratospheric 45 mbar wind velocity for the period from 1951 to 1991, ◇, January-February mean values (a) Unstratified data. (b) January-February data for winters only in the west phase of the QBO. (c) January-February data for winters only in the east phase of the QBO.

[*Varotsos*, 1989], since for all of these studies data stratified by the QBO phase also show correlations with the 11-year solar cycle.

3. UNIQUENESS OF SOLAR ACTIVITY FORCING FOR DECADAL TIME SCALE VARIATIONS

It was pointed out by *Baldwin and Dunkerton* [1989], *Teitelbaum and Bauer* [1990], *Dewan and Shapiro* [1991] and *Salby and Shea* [1991] that the interval of about 33 years, over which the correlation of stratified winter stratospheric and tropospheric temperatures with the solar cycle holds, is too short to uniquely identify the 11-year solar cycle as the forcing function; in fact, simulated forcing functions with periods from 8 to 15 years with optimized phases show correlation coefficients which are just as high. The suggestion is that because the atmospheric variability is not uniquely identified with 11-year solar cycle, there is no justification for considering that a physical mechanism connects the atmosphere and the solar variability. However, this argument is invalidated by the fact that although several inputs to the atmosphere from the sun, varying on the 11-year cycle, have been identified (solar ultraviolet, solar visible-infrared, MeV particles, GeV particles, electric fields from the solar wind-magnetosphere-ionosphere interaction), no plausible nonsolar inputs of an 8- to 15-year periods have been identified. For a discussion of solar inputs, see the *National Research Council* [1982] report. The lack of uniqueness does not mean that solar forcing is excluded, only that it is not confirmed. An 11-year solar forcing would account for the high correlations with simulated periods ranging from 8 to 15 years and is thus the logical choice to begin a search for mechanisms.

The problem of nonuniqueness is not present for correlations found in several sets of unstratified atmospheric data that extend over periods much longer than 33 years. Summertime atmospheric temperatures in the central United States correlate well with the solar cycle, as shown in Figures 4 and 5 (after *Chang and Lau*, [1990]; and *Labitzke and van Loon*, [1992], respectively). The Kansas City temperature variations were previously shown to be representative of a large area of the central United States [*Chang and Wallace*, 1987], as also are the Charleston temperature variations [*Labitzke and van Loon*, 1992]. The two figures combined represent a 95-year period showing the correlation. The interval between the early 1960s to the mid-1970s, when the amplitude of the atmospheric variation was low and the correlation with the solar cycle was not present, can be attributed to the effects on climate of the volcanic aerosols from the Mt. Agung eruption [*Labitzke and Naujokat*, 1983; *Newell*, 1970]. Figure 5 shows that the atmospheric temperature variation returned to being in phase with the solar cycle following the decay of the Mt. Agung-associated transient. Apart from this period there were six cycles of atmospheric temperature in phase with the solar cycle and two in quadrature. Some cycles in quadrature are to be expected since other sources of variability exist, as part of a red noise continuum due to sea surface temperature change and internal atmospheric variability, in addition to volcanism. Another long-term data set showing a good correlation with solar variability is that of north Atlantic winter storm track latitudes over a 67-year period [*Tinsley and Deen*, 1991]. Four cycles are in phase, and although two cycles are in quadrature, the associated storm frequency and surface temperature variations remain in phase. The study of 100 years of north Atlantic mean sea level pressure by a principal component analysis [*Kelley*, 1977] revealed significant peaks

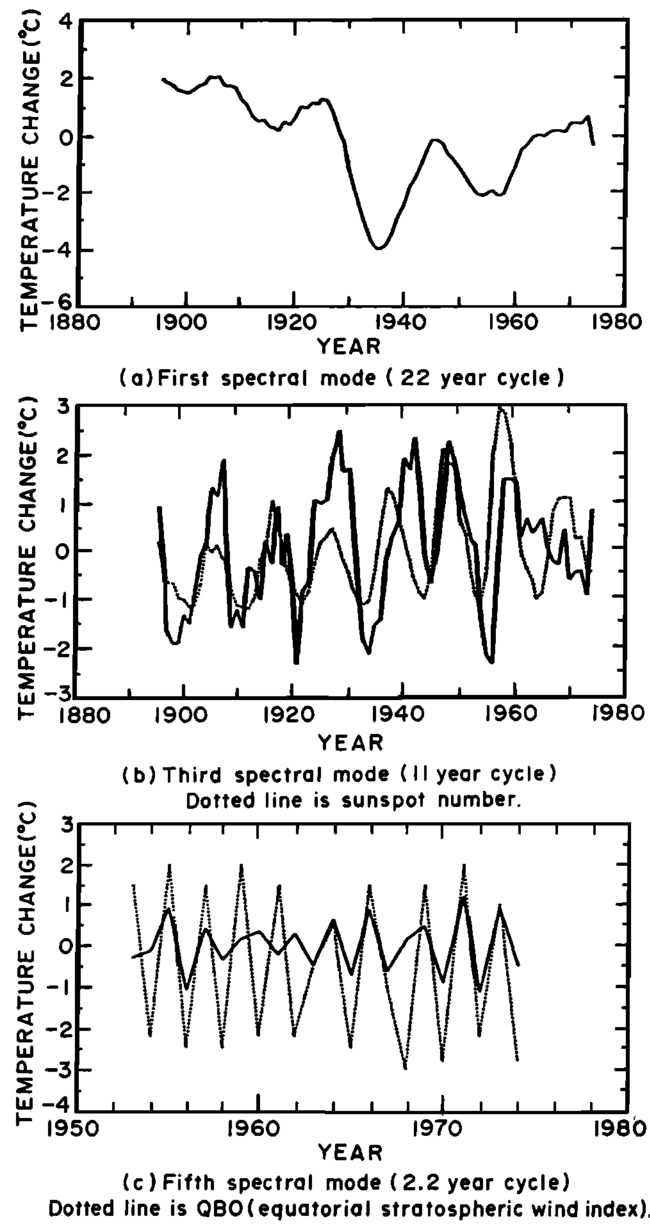

Fig. 4. Spectral components of mean summer (June, July, August) temperatures at Kansas City, from singular spectral analysis. The vertical scale shows the departure of the temperature from the mean. After *Chang and Lau* [1990].

centered on 11 and 2.2 years. A maximum entropy analysis of 102 years of data on Atlantic tropical cyclones [*Cohen and Sweester*, 1975] showed that for the range of periods from 6 to 40 years the number of tropical cyclones/season, and the length of the season, had strongest peaks at 11.3 and 10.9 years respectively. There were also smaller peaks at 22 and 21.2 years respectively. A study of 250 years of ice accumulation data from Mt. Logan, Yukon [*Holdsworth* et al., 1989] showed prominent peaks in accumulation rate at 3.8, 11.3, and 21 years. The 3.8-year peak may be identified with the el Niño-Southern Oscillation period. It is difficult to attribute the 11- and 22-year periods in the above data sets to anything other than solar forcing.

4. UNIQUENESS OF SOLAR ACTIVITY FORCING ON THE DAY-TO-DAY TIME SCALE

4.1. *Forcing by Changes in Atmospheric Ion Production*

Tinsley and Deen [1991] found correlations between changes in the 500 m-bar vorticity area index (a measure of the intensity

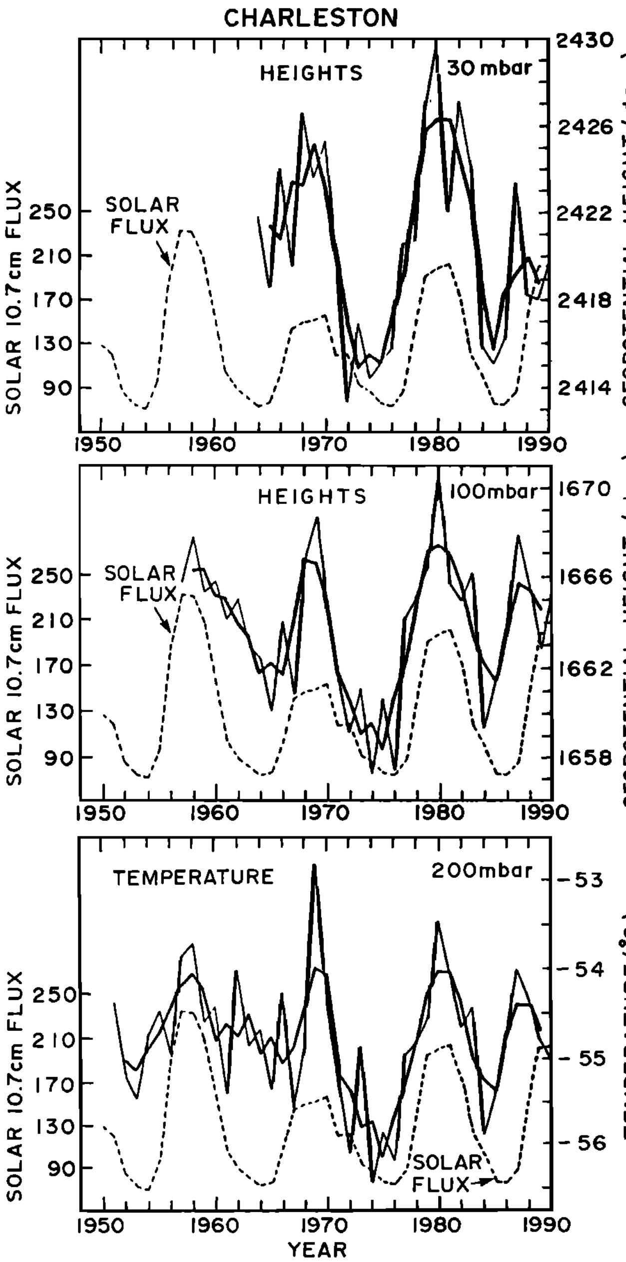

Fig. 5. Time series of the 200-mbar temperature and 100- and 30-mbar geopotential height in July-August and of the 10.7-cm solar flux. Heavy lines are 3-year running means. The period of poor correlation in the mid-1960s here and in Figure 4 follows the Mt. Agung volcanic eruption. After *Labitzke and van Loon* [1992].

of cyclonic disturbances) and changes in neutron monitor count rates (a proxy for the rate of ion production by cosmic rays in the upper troposphere). The set of 108 events studied were at times of Forbush decreases in the flux of galactic cosmic rays, caused by magnetic shock waves in the highly disturbed solar wind. The correlations were present when the set of events was divided in four different ways: with respect to the first 16 years and next 15 years, with respect to the first and second halves of winter, with respect to east and west QBO phase winters, and with respect to larger and smaller Forbush decreases (larger and smaller apparent responses). The correlations were not present when a set of key days of large 10.7 cm solar flux variations, representing variable solar photon inputs into the atmosphere, were used in the analysis. Therefore, the apparent responses were uniquely identifiable with solar wind forcing.

4.2. *Forcing by Changes in Polar Cap Ionospheric Potential*

We now describe a completely independent set of correlations on the day-to-day time scale, which are found for quiet solar wind conditions with relatively little change in cosmic ray flux.

Figure 6 shows the variation of ionospheric potential along a dusk-dawn (1800-0600 hours) meridian through the northern polar region. The curves are from the analytical model of *Hairston and Heelis* [1990], which is derived from an empirical fit to a large data base of measurements made with the DE-2 satellite, and are consistent with many other such measurements. The three curves correspond to the solar wind azimuthal magnetic field component By having values of +7, 0, and -7 nT, for a maximum horizontal dawn-dusk potential difference, Φ, of 80 kV. This value for Φ is typical for average conditions if the component Bz of the solar wind magnetic field is negative (southward), with the actual value being a function of both Bz and the solar wind velocity, V [*Reiff and Luhman*, 1986]. For these applications, By and Bz are expressed in a solar-terrestrial coordinate system, known as the geocentric solar magnetospheric (GSM) system [*Crooker and Siscoe*, 1986]. It can be seen that within 5° of the pole the ionospheric potential rises and falls by 40 Kv, as By changes from -7 to +7 nT and back to -7 nT.

Figure 7 shows Σ, the average of the ionospheric potentials over areas of both the northern and southern polar caps. Specifically, for 7*a* the average is over the circular regions of radius 10° magnetic colatitude (2200 km in diameter, centered on the magnetic poles) and for Figure 7*b* it is the zones between 10° and 15° magnetic colatitude. The heavy solid lines are for the northern polar cap with Φ = 80 kV, and they each include three points corresponding to the area averages associated with the three curves for Figure 6. The lighter solid lines are for the northern polar cap, with values of Φ equal to 50 and 120kV. The dashed curves show the averaged potential for the same values of Φ in the southern polar cap. Note that the area-averaged potentials Σ are asymmetric with By because of the asymmetry in the convection pattern as a function of By as shown in Figure 6. The opposite variations in the northern and southern polar caps result from the finding that there is no significant difference between convection patterns in the north when By is positive and in the south when By is negative. This asymmetric distribution with By is also seen in ground-based measurements of ionospheric current [*Friis-Christensen et al.*, 1972; *Mansurov et al.*, 1974; *Svalgaard*, 1974] and of electric field [*Holt et al.*, 1987]; the studies by *Mansurov et al.* [1974] and *Svalgaard* [1974] show its opposite behavior in the two hemispheres.

It was found by *Mansurov et al.*, [1974] that the surface pressure at Mould Bay and Dumond d'Urville, two stations about 10° from the north and south 'invariant' magnetic poles respectively, varied by about 4 mbar between periods when the solar wind Bx value was positive and when it was negative and that this variation was opposite in the Antarctic and the Arctic. The magnetic coordinate system used to define the *Hairston and Heelis* [1990] model and the curves of Figure 6 has its polar axis passing through the 'invariant' magnetic poles. A result consistent with that of *Mansurov et al.* [1974] was found by *Page* [1988, 1989], who compared daily average surface pressures at Thule, Greenland, with those at McMurdo, Antarctica, for Bx values in 1-nT intervals between -7 and +7 nT over the period 1964-1974. These stations are also about 10° from the 'invariant' magnetic poles. Values of the solar wind magnetic field component By are highly correlated with the values of Bx as a result of the field geometry [*Hirschberg*, 1969], and the average field 'garden hose' angle of 45° defines a constant of proportionality of -1.0.

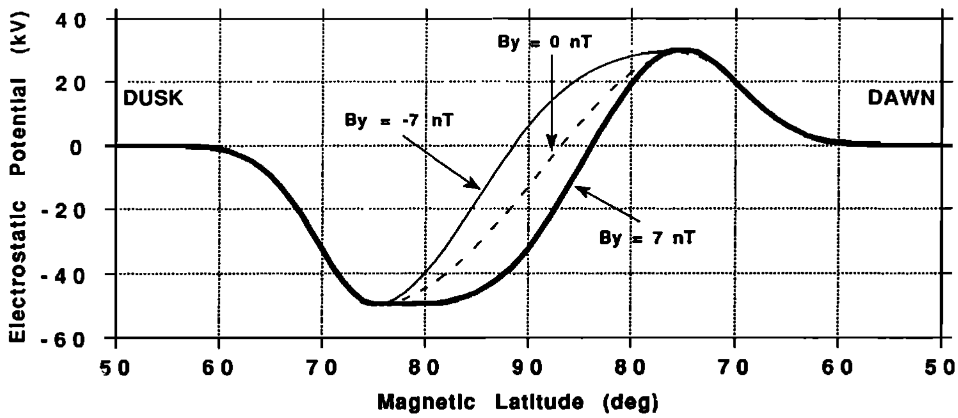

Fig. 6. Average polar cap ionospheric potential variations measured along the dawn-dusk line in the northern hemisphere with *Bz* negative and for a 80 kV total horizontal ('dawn-dusk') potential difference, Φ, for three *By* values. In the southern hemisphere the variations correspond to those in the northern hemisphere but with the sign of *By* reversed.

Therefore the apparent responses to changes in *Bx* can also be interpreted as an apparent response to *By* changes. In Figure 7*c* we replot the results of Page [1989] in the same format as Figure 7*a* and 7*b*, with *By* replacing -*Bx* the pressures converted to millibars, and with estimated error bars added. We also replot the results of *Mansurov et al.* [1974] as solid circles for Mould Bay and open squares for Dumond d'Urville, with the mean pressures for the stations taken as 972.5 and 979.5 mbar, respectively, for the purposes of clarity in plotting the differences on the figure. The error bars on pressure represent *estimated* deviations *of* the mean, obtained from the pressure distributions of *Mansurov et al.* [1974], which show *measured* average deviations of individual data points *from* the mean of 10 mbar. *Page* [1989] utilized a total of 2495 events in 14 bins. Taking into account the bimodal distribution of occurrence of daily average *By* values measured for the years 1974 and 1982, we calculated the variable error bars for pressure shown. The mean positive and mean negative *By* values both had magnitudes of 3.0 $\pm$ .25 nT in the solar minimum year 1974 and the solar maximum year 1982, and so we used this value to represent 1964. We assumed a persistence of three days for both the pressure and *By* variations in calculating the deviations of the means. The results with estimated errors for *Page*'s [1989] data are consistent with a linear variation of pressure with *By*, with a slope of -0.2 $\pm$ 0.1 mbar/nT for Thule (Arctic), and a slope of +0.2 $\pm$ 0.1 mbar/nT for McMurdo (Antarctic). For the data of *Mansurov et al.*, [1974], larger slopes of -0.67 $\pm$ 0.3 mbar/nT for Mould Bay (Arctic) and +0.67 $\pm$ 0.3 mbar/nT for Dumond d'Urville (Antarctic) are found.

The correlations described above, of Σ with *By* on the one hand, and of tropospheric pressure with *By* on the other, are so similar as to leave little reason to interpret these as chance correlations. We note that (1) a systematic variation of surface pressure with *By* has been found for four different locations, over two different time intervals; and (2) within the polar caps the variations of pressure with *By* are opposite in the southern hemisphere to the variations in the northern hemisphere, as are the variations of Σ with *By*.

These correlations were found for a small fraction of all the data now available, and there is a need to test for their persistence in more recent and comprehensive measurements of pressure and geopotential height which extend across both polar caps. Also, the ionospheric potentials are strongly affected by the dawn-dusk potential difference, Φ, which depends on the *Bz* (GSM) component of the solar wind magnetic field. Because of the changing orientation of the GSM coordinate axes on an annual cycle, *Bz* (GSM) shows a correlation with *By* in some seasons, and an anticorrelation in others. Therefore it is preferable to test for the correlation of pressure (and geopotential height) with the area averaged potential Σ rather than with *By*, with Σ calculated from both Φ and *By* (GSM).

5. DISCUSSION OF A POSSIBLE MECHANISM

The average ionospheric potential with respect to the earth is positive and about 250 Kv. Most of this potential difference appears across the lowest 10 km of the atmosphere [*Roble and Tzur*, 1986] giving rise to the vertical electric field in the troposphere, with efficient downward mapping of the ionospheric horizontal variations for areas of scale size greater than a few hundred kilometers. The satellite measured changes in the ionospheric potential by ca. 40 kV represent a 10-20% change in the ionosphere-earth potential difference and thus a 10-20% change in the vertical tropospheric electric field, which must co-vary with Σ. The large-scale electric field in the troposphere produces a downward current, which meets an obstacle in clouds because of their low conductivity, producing boundary polarization charge layers at the tops and bottoms of the clouds and a high polarization electric field in between [*Beard and Ochs*, 1986]. The production of these charge layers proceeds by cloud droplets of radius R capturing charge up to a maximum Q in a growing field of magnitude E, where ϵ_0 is the permittivity of free space and Q is given by

$$Q = 12\pi\epsilon_0 R^2 E$$

which amounts to 180 elementary charges for a 30-μm-radius droplet in a field of 100 V/m. The process steadily increases the amount of charge in the layer, and the polarization electric field E, and consequently the amount of charge attained per droplet, until the atmospheric current is continuous through the cloud or the process is interrupted by transport effects. The rate at which the charging proceeds depends on the atmospheric current, which, in turn depends on (1) the atmospheric ion concentration and thus on the cosmic ray flux, and (2) the local ionospheric potential. The charge on a supercooled droplet at cloud top is therefore likely to vary as a function of the product of the cosmic ray flux and the local ionospheric potential.

The vertical atmospheric electric fields at cloud top are of the order of 10 V/m, amplified by another order of magnitude in the polarization electric field within the cloud. As clouds develop and the polarization field increases, large fluctuating fields are found

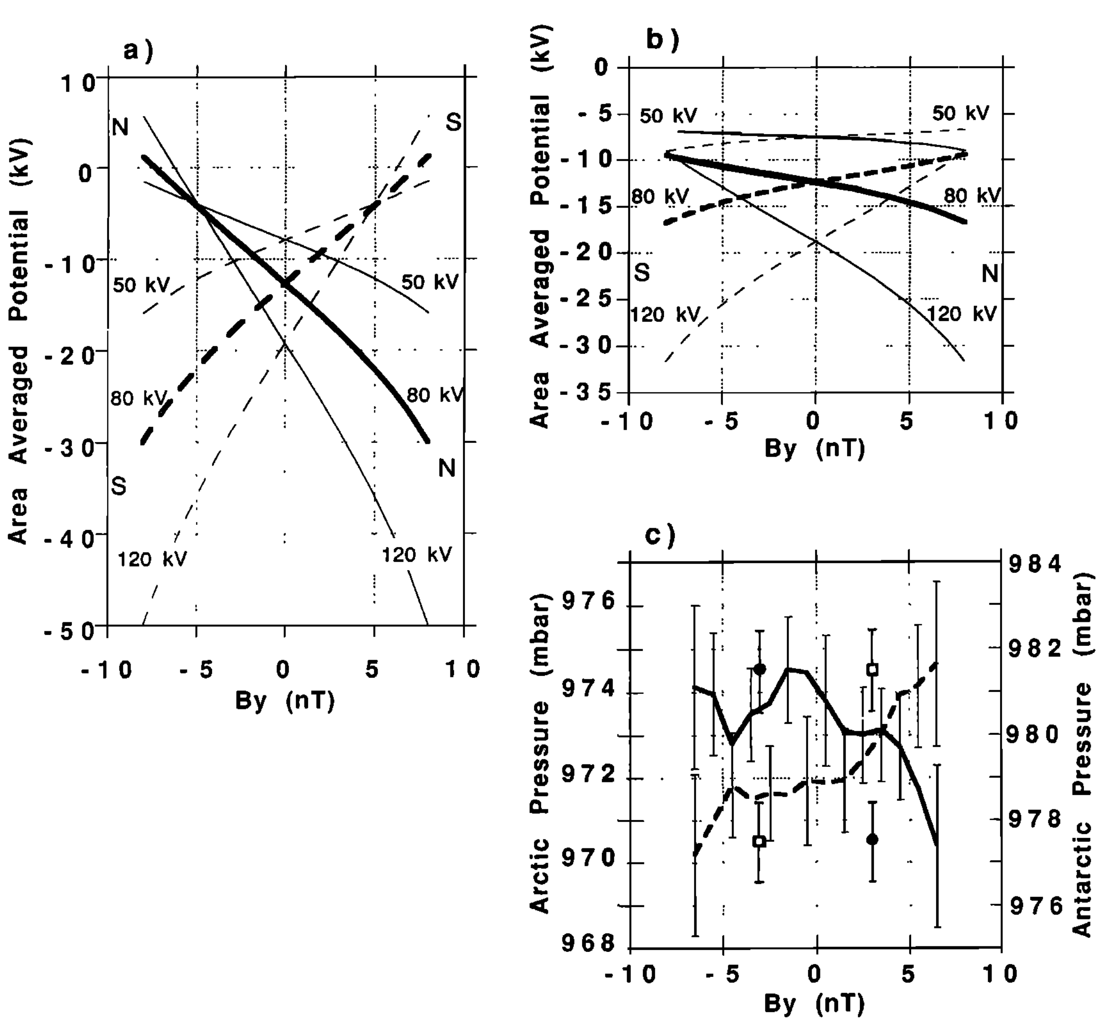

Fig.7. (*a*) Variation of area averaged ionospheric potential Σ with *By* for three values of the dawn-dusk potential difference, Φ, for northern and southern hemispheres for the areas of radius 10° magnetic colatitude. Solid curves, northern hemisphere values, dashed curves, southern hemisphere values. (*b*) Variation of Σ for the zones between 10° and 15° colatitude. (*c*) Variation with *By* of surface pressure at Arctic and Antarctic stations, replotted with -*Bx* replaced by *By*, with pressure in millibars, and with error bars estimated, as discussed in the text. Solid line, Thule (north); dashed line, McMurdo (south) (after *Page* [1989]. Solid circles, Mould Bay (north); open squares, Dumond d'Urville (south) (after *Mansurov et al.* [1974]).

to be present also. Although the atmospheric and polarization fields remain small compared with these fluctuating fields, in the context of section 4 we are considering averages over regions hundreds of kilometers across. The points in Figure 7c are averages of 50 days or more of measurements. In addition, the amplitudes of the fluctuating cloud fields may scale with the ambient atmospheric field. Although the understanding of the cloud- charging process is still in an exploratory stage [*Beard and Ochs*, 1986], it appears that for the cloud stage of interest here, i.e., before significant amounts of ice are produced, the electric field fluctuations are produced by convection and turbulence, redistributing both the atmospheric charge density (as a result of the constant vertical current in the presence of vertical gradients in atmospheric conductivity) and the polarization charge density. Therefore, a spectrum of fluctuations would be generated with overall scaling for amplitude proportional to the ambient vertical atmospheric electric field (in the absence of cosmic ray variations). It should be noted that we do not intend to imply that such charging processes are responsible for lightning electric fields, since after ice formation takes place other charge separation processes become important [*Beard and Ochs*, 1986].

If the above scenario is generally correct, the contributions to droplet charging from both the average and the strongest cloud fields would be responsive to the product of the cosmic ray flux and the local ionospheric potential. The electrofreezing mechanism postulates that variations in the amount of such charge affect the rate of initial ice generation at the tops of clouds. Ice generation is not well understood, although it is the first step in the standard Wegener-Bergeron-Findeison mechanism for precipitation. In their recent study, *Hobbs and Rangno* [1990] suggested that contact ice nucleation at the tops of cumuliform clouds occurs first and is followed by deposition or condensation-freezing nucleation. There is at least one process by which electrostatic charging of cloud droplets and aerosols will enhance the contact ice nucleation rate, and quite plausibly two. The process already recognized is the increase in collection efficiency for aerosols (acting as ice nuclei) by charged droplets compared with that by uncharged droplets. From models, the effect is an increase by up to an order of magnitude for collection of aerosols between 10^{-2} and 1 μm in radius by droplets of a few tens of μm in radius with typical cloud charges [*Wang et al.*, 1978]. Measurements of the effect show an increase by up to two orders of magnitude [*Barlow and Latham*, 1983]. The second process is that of electrostatic charge effects on the physics of nucleation itself, for which laboratory evidence has been reviewed by *Tinsley and Deen* [1991]. The most recent laboratory evidence is that of *Gavish et al.* [1992], who reported on a comparison of the ice-nucleating ability of polar and nonpolar crystals that were otherwise closely matched, with neither having a structural match to ice. The polar crystals were much more efficient nucleators than the nonpolar crystals were. The ice nucleation was observed to occur at submicroscopic cracks in the crystal, which suggests that it is the microscale electric fields, due to electrostatic charges that appear on opposite walls of cracks in polar crystals, that are the significant physical agent ordering water molecules (or embryonic ice crystals below the critical size) and promoting ice nucleation. Therefore, in the atmosphere, the microscopic electric field that exists at the moment of contact of oppositely charged supercooled water droplets and aerosols may similarly promote ice nucleation.

The successive steps in the chain of processes linking changes in ice nucleation with changes in atmospheric dynamics and/or temperature may be different in winter and summer. Clouds are colloidal suspensions which are unstable gravitationally, and they are also unstable thermodynamically to changes of phase when above the freezing altitude. When the droplets are induced to freeze and/or grow and coalesce and precipitate before they evaporate, there are large effects on atmospheric dynamics because of net latent heat release and consequent changes in vertical air motions, which affect atmospheric vorticity and atmospheric pressure. There may also be effects due to changes in cloud radiative forcing. The electrofreezing process will change the particle size distribution even in those clouds in which the ice crystals do not grow large enough to affect precipitation, and the process will affect the water content as well as cloud albedo in those clouds that do precipitate. There may also be effects due to water vapor radiative forcing, as a result of changes in the amount of water vapor that remains in the atmosphere when clouds dissipate after ice crystals grow large enough to affect precipitation. Since water vapor is the most important greenhouse gas (it is 100 times more abundant than CO_2 at low latitudes and low altitudes), small systematic changes in its concentration could have significant effects on climate. Although the theory of all of these processes in the context of real clouds is still in an exploratory stage, and although other processes may be important, we suggest that the rate of cloud droplet charging affects the rate of initial ice nucleation and ultimately atmospheric dynamics and/or temperature. In this way it is possible to account for the observed correlations of atmospheric dynamics and temperature, both with cosmic ray flux changes on the day-to-day and decadal time scales and with electric field changes on the day-to-day time scale.

For winter conditions, the temperature contrast between polar air masses and relatively warm water, as well as the presence of a well developed baroclinic instability, favors the chain of processes progressing from ice nucleation through the seeder-feeder process [*Rutledge and Hobbs*, 1983]. The steps include the release of latent heat, the increase in vertical motions within cloud systems, and consequent changes in vorticity and surface pressure. In warm-core winter cyclones, the final step is the conversion of the linear kinetic energy of the general circulation to eddy kinetic energy, producing waves that propagate out of the region and changes in the general circulation, as discussed in *Tinsley et al.*, [1989] and *Tinsley and Deen* [1991]. An overview of the scaling of energy between droplet charging and atmospheric dynamics is as follows. Changes in the mean tropospheric temperature by 6°C, or in atmospheric vorticity related to surface pressure changes by a few millibars, are equivalent to a redistribution of atmospheric energy by about 10^{-3} W cm^{-2}. The production rate of ions in the upper troposphere is about 10 cm^{-3} s^{-1} [*Neher*, 1971], and so in a layer 1 m thick at the tops of clouds about 10^3 ions are produced per second per column of 1 square centimeter cross section in the layer. The typical downward flux of ice crystals in fall streaks and in the model of *Rutledge and Hobbs* [1983] is about 1 cm^{-2} s^{-1}, so that the above values would be consistent with 1 in 10^3 charged aerosols actually causing electrofreezing, assuming that all ions attach to aerosols. This flux of seeder crystals produced a doubling of the precipitation rate in warm frontal rainbands in the model. If each ice crystal resulted in a 1-mm-diameter water droplet leaving the atmosphere, rather than the water being reevaporated, the net latent heat released to the atmosphere is about 1 J per drop, or 1 W cm^{-2}. We can reduce this energy flux by a factor of 10 since we are tracking a 10% change in the input and further reduce it by a factor of 10^2 for the intermittent nature of the precipitation in space and time, and we can still account for 10^{-3} W cm^{-2}. This represents both the day-to-day changes in tropospheric dynamics in winter and the changes in winter storms on the decadal time scale as discussed by *Tinsley and Deen* [1991].

For the summer variations of Figures 4 and 5, the effects of radiative forcing as consequences of electrofreezing may be more important. A change in high level cloud opacity by 5% would change the heating rate in the column below of the order of 0.03°C/day [*Dickinson*, 1975], so that in 2 months a 2°C surface temperature change would result, in agreement with the results in Figure 4. This is neglecting any contributions due to changes in circulation.

The explanation of the stratospheric variations shown in Figure 1, and the role of the QBO in them remains a puzzle. The effects occur in January and February, when the vortex is unstable to small dynamic or temperature perturbations. The region concerned is the upper stratosphere where very little supercooled water is formed, and so effects propagating up from the troposphere and additional effects due to changes in stratospheric ionization should be considered. The amount of energy required say to heat the region above the altitude of the 40 mbar level by 20°C is small compared with that involved in the decadal tropospheric changes (e.g., about 10% of the energy involved in the change of surface temperature by 6°C in the eastern United States, as found by *van Loon and Labitzke* [1988]. The amount just to trigger stratospheric warming would be considerably smaller. Studies have been carried by *Dameris and Ebel* [1990], *O'Sullivan and Salby* [1990], and *Balachandran et al.* [1991] on the propagation of planetary waves, originating in the troposphere at low latitudes, to the high-latitude stratospheres and their effects on stratospheric warming there. They found that the effects were greater during east phase QBO conditions than during west phase conditions. Taken with greater planetary wave generation by intensification of winter cyclones at solar minimum compared with solar maximum, there is the possibility of explaining the east phase variation of the relationships in Figure 1. The west phase variation would have to be explained separately. In this context it may be important that the upper boundary condition for propagation of waves in the stratosphere is subject to significant 11-year cycles due to the solar ultraviolet variability. QBO effects on stratospheric water vapor and minor chemical concentrations [*Chipperfield and Gray*, 1992] that may be carried into the polar vortex by meridional stratospheric circulation also remain to be explored, in the context of possible effects of stratospheric ionization on the nucleation of stratospheric sulfate aerosols [*Dickinson*, 1975] and on the formation and rate of sedimentation of type I polar stratospheric clouds [*Dye et al.*, 1992; *Arnold et al.*, 1992]. These may in turn affect polar ozone concentrations and the temperature structure. Although the above speculative discussion may show little similarity to the eventual explanation of the relationships in Figure 1, its purpose is to draw attention to the uncertainties in our understanding the polar stratosphere, and the effect on them of physical changes related to QBO phase and solar inputs, which leave adequate room for an explanation by some such combination of physical and chemical processes. The complexities of the system are such that the explanation is unlikely to be found without a serious research effort directed toward finding it.

6. CONCLUSIONS

The aliasing effects of annual sampling of a suggested atmospheric forcing by the QBO alone provide an inadequate explanation of the reported correlations of winter stratospheric temperature and other atmospheric parameters, stratified by the QBO, with the 11-year solar cycle. In long time series of unstratified climate data, the solar periods of 11 and 22 years are prominent, as are longer solar periods, and support the concept of forcing on these time scales as being due to solar activity. Day-to-day correlations between solar wind magnetic field changes and atmospheric dynamic variations are found for two independent inputs to atmospheric electricity and support a mechanism (electrofreezing) in which the solar wind affects electrostatic charging of supercooled water droplets and aerosols at the tops of clouds, thereby increasing the rate of ice nucleation. This in turn would affect latent heat release, vertical motions, storm dynamics, and the general circulation and would affect higher levels of the atmosphere through upward propagation of gravity and planetary waves. For summertime conditions, the effects of changes in radiative forcing as a result of electrofreezing may be more important. Much more work is required before these mechanisms can be considered to have a secure basis in laboratory experiment and quantitative atmospheric modeling.

Acknowledgments. This work has been supported by the National Science Foundation Division of Atmospheric Sciences under grant ATM-8902207 and by the Division of Polar Programs under grant DPP-9208937.

REFERENCES

Arnold, F., K. Petzold, and E. Reimer, On the formation and sedimentation of stratospheric nitric aerosols, implications for polar ozone destruction, *Geophys. Res. Lett, 19,* 667, 1992.

Balachandran, N. K., R. A. Plumb, R. Suozzo, and D. Rind, The QBO and stratospheric warming - model results, *J. Geomagn. Geoelect., 43,* (Supplement), 741, 1991.

Baldwin, M. P., and T. J. Dunkerton, Observations and statistical simulations of a proposed solar cycle/QBO/weather relationship, *Geophys. Res. Lett., 16,* 863, 1989.

Barlow, A. K., and J. Latham, A laboratory study of the scavenging of sub-micron aerosol by charged raindrops, *Q. J. R. Meterol. Soc., 109,* 763, 1983.

Barnston, A. G., and R. E. Livezey, Statistical prediction of January-February mean northern hemisphere lower tropospheric climate from the 11 year solar cycle and the southern oscillation for west and east QBO phases, *J. Clim., 4,* 249, 1991.

Beard, K. V. K., and H. T. Ochs, Charging mechanisms in clouds and thunderstorms, in *The Earth's Electrical Environment*, p, 114, National Research Council, National Academy of Sciences, Washington, D.C., 1986.

Chang, F.-C., and K.-M. Lau, Natural variability in summertime droughts over the United States Great Plains, preprint volume, p., 181, *Bull. Am. Met. Soc.* Feb., 1990.

Chang, F.-C., and J. M. Wallace, Meteorological conditions during heat waves and droughts in the United States Great Plains, *Mon. Weather Rev., 115,* 1253, 1987.

Chanin, M.-L., P. Keckhut, A. Hauchecorne and K. Labitzke, The solar activity-Q.B.O. effect in the lower thermosphere, *Ann. Geophys, 7,* 4-63, 1959.

Chipperfield, M. P., and L. J. Gray, Two-dimensional model studies of the interannual variability of trace gases in the middle atmosphere, *J. Geophys. Res., 97,* 5963, 1992.

Cohen, T. J., and E. I. Sweester, The 'spectra' of the solar cycle and of data for Atlantic tropical cyclones, *Nature, 256,* 195, 1975.

Crooker, N. U., and G. L. Siscoe, The effect of the solar wind on the terrestrial environment, in *Physics of the Sun,* vol III, edited by P. A. Sturrock, p. 193, D. Reidel, Norwell, Mass, 1986.

Dameris, M., and A. Ebel, The quasibiennial oscillation and major stratospheric warming, a three dimensional model study, *Ann. Geophys.,8,* 8, 79, 1990.

Dewan, E. M., and R. Shapiro, Are sunspot-weather correlations real? *J. Atmos. Terr. Phys., 53,* 171, 1991.

Dickinson, R. E., Solar variability and the lower atmosphere, *Bull. Am. Meteorol. Soc., 56,* 1240, 1975.

Dye, J. E., D. Baumgardner, B. W. Gandrud, S. R. Kawa, K. K. Kelly, M. Lowenstein, G. V. Ferry, K. R. Chan and B. L. Gary, Particle size distributions in Arctic polar stratospheric clouds, growth and freezing of sulphuric acid droplets, and implications for cloud formation, *J. Geophys. Res.,97,* 8015, 1992.

Friis-Christensen, E., K. Lassen, J. Wilhjelm, J. M. Wilcox, W. Gonzalez, and D. S. Colburn, *J. Geophys. Res. 77,* 3371, 1972.

Gavish, M., J.-L. Wang, M. Eisenstein, M. Lahav, and L. Leiserowitz, The role of crystal polarity in α-amino acid crystals for induced nucleation of ice, *Science, 256,* 815-818, 1992.

Gray, L. J., and J. A. Pyle, A two dimensional model of the quasibiennial oscillation of ozone, *J. Atmos. Sci., 46,* 203, 1989.

Hairston, M. R., and R. A. Heelis, Model of the high latitude ionospheric convection pattern during southward interplanetary magnetic field, using DE 2 data, *J. Geophys. Res., 95,* 2333, 1990.

Hirschberg, J., The interplanetary field during the rising part of the solar cycle, *J. Geophys. Res., 74,* 5814, 1969.

Hobbs, P. V., and A. R. Rangno, Rapid development of high ice particle concentrations in small polar maritime cumuliform clouds, *J. Atmos. Sci., 47,* 2710, 1990.

Holdsworth, G., H. R. Krouse, M. Nosal, M. J. Spenser and P. A. Mayewski, Analysis of a 290-year-net accumulation time series from Mr. Logan, Yukon, *Snow cover and glacier variation,* IAHS Publ. # 183, Ed. S. Colbeck, p. 71. Wallingford, Oxfordshire.

Holt, J. M., R. H. Wand, J. V. Evans, and W. L. Oliver, Empirical models for the plasma convection at high latitudes from Millstone Hill observations, *J. Geophys. Res., 92,* 203-212, 1987.

Holton, J. A., Possible physical mechanisms: dynamic coupling, in *Solar Variability, Weather and Climate*, p. 79, National Academy of Sciences Press, Washington, D.C., 1982.

Kelley, P. M. Solar influence on north Atlantic mean sea level pressure, *Nature, 269,* 320, 1977.

Labitzke, K., Sunspots, the QBO and the stratospheric temperature in the north pole region, *Geophys. Res. Lett., 14,* 535, 1987.

Labitzke, K., and B. Naujokat, On the variability and on trends of the temperature in the middle stratosphere, *Contrib. Atmosph. Phys., 56,* 495, 1983.

Labitzke, K., and H. van Loon, Associations between the 11-year solar cycle, the QBO and the atmosphere, I. The troposphere and the stratosphere of the northern hemisphere in winter, *J. Atmos. Terr. Phys., 50,* 197, 1988.

Labitzke, K., and H. van Loon, Association between the 11 year solar cycle and the atmosphere. Part V: Summer, *J. Clim.*, *5*, 240, 1992.

Mansurov, S. M., L. G. Mansurova, G. S. Mansurov, V. V. Mikhnevich, and A. M. Visotsky, North-south asymmetry of geomagnetic and tropospheric events, *J. Atmos. Terr. Phys*, *36*, 157, 1974.

Marcz, F., Atmospheric electricity and the 11 year solar cycle associated with QBO, *Ann. Geophys.*, *8*, 525, 1990.

Markson, R., Solar modulation of atmospheric electrification and possible implications for the Sun-weather relationship, *Nature*, *273*, 103, 1978.

Mason, S. J., and D. D. Tyson, The modulation of sea surface temperature and rainfall associations over Southern Africa with solar activity and the Quasi-Biennial Oscillation, *J. Geophys. Res.*, *97*, 5847, 1992.

National Research Council Panel on Solar Variability, Weather, and Climate, *Solar Variability, Weather and Climate*, National Academy of Sciences Press, Washington, D. C., 1982.

Neher, H. V., Stratospheric temperature change from the Mt. Agung volcanic eruption of 1963. *J. Atmos. Sci. 27*, 977, 1970.

Newell, R. E., Stratospheric temperature change from the Mt. Agung volcanic eruption of 1963, *J. Atmos. Sci.*, *27*, 977, 1970.

Newkirk, G. A., The nature of solar variability, in *Solar Variability, Weather and Climate*, p. 33, National Research Council, National Academy of Science Press, Washington, D. C., 1982.

Ney, E. P., Cosmic radiation and the weather, *Nature*, *183*, 451, 1959.

O'Sullivan, D., and M. L. Salby, Coupling of the quasi-biennial oscillation and the extratropical circulation in the stratosphere through planetary wave transport, *J. Atmos. Sci.*, *47*, 650, 1990.

Page, D. E., The Interplanetary magnetic field and sea level polar atmospheric pressure (abstract), *Eos Trans. AGU*, *69*, 1353-1988.

Page, D.E., The interplanetary magnetic field and sea level polar atmospheric pressure, in *Workshop on Mechanisms for Tropospheric Effects of Solar Variability and the Quasi-Biennial Oscillation*, edited by S. K. Avery and B. A. Tinsley, p. 227, University of Colo., Boulder, Colo., 1989.

Reiff, P. H., and J. G. Luhman, Solar wind control of the polar cap voltage, in *Solar Wind Magnetosphere Coupling*, edited by Y. Kamide and J. Slavin, p. 453, Terra-Reidel, Tokyo, 1986.

Roble, R. G., and I. Tzur, The global atmospheric-electrical circuit, in *The Earth's Electrical Environment*, p. 206, National Academy of Sciences Press, Washington, D. C. 1986.

Rutledge, S. A., and P. V. Hobbs, The mesoscale and microscale structure and organization of clouds and precipitation in midlatitude cyclones, VIII, a model for the "Seeder Feeder" process in warm frontal rainbands, *J. Atmos. Sci.*, *40*, 1185, 1983.

Salby, M. L., and D. J. Shea, Correlations between solar activity and the atmosphere: An unphysical explanation, *J. Geophys Res.*, *96*, 22,579, 1991.

Svalgaard, L., The relation between the azimuthal component of the interplanetary magnetic field and the geomagnetic field in the polar caps, in *Correlated Interplanetary and Magnetoshpheric Observations*, edited by D. E. Page, p. 61, D. Reidel, Norwell, Mass., 1974.

Teitelbaum, H., and P. Bauer, Stratospheric temperature eleven years variations: Solar cycle influence or stroboscopic effect? *Ann. Geophys.*, *8*, 239, 1990.

Tinsley, B. A., Forcing of the troposphere and stratosphere by MeV-GeV particle flux variations: Observations and a new cloud microphysical mechanism (abstract), *Eos Trans AGU*, *71*, 1251, 1990.

Tinsley, B. A., and G. W. Deen, Apparent tropospheric response to MeV-GeV particle flux variations: A connection via electrofreezing of supercooled water in high-level clouds? *J. Geophys. Res.*, *96*, 22,283, 1991.

Tinsley, B. A., G. M. Brown, and P. H. Scherrer, Solar variability influences on weather and climate; possible connections through cosmic ray fluxes and storm intensification, *J. Geophys. Res.*, *94*, 14,783, 1989.

van Loon, H., and K. Labitzke, Association between the 11 year solar cycle, the QBO, and the atmosphere, Part III, surface and 700 mb on the northern hemisphere in winter, *J. Clim.*, *1*, 905, 1988.

Varotsos, C., Comment on connection between the 11-year solar cycle, the QBO and total ozone, *J. Atmos. Terr. Phys.*, *51*, 367, 1989.

Venne, D. E., and D. G. Dartt, An examination of possible solar-cycle QBO effects in the northern hemisphere troposphere, *J. Clim.*, *3*, 272, 1990.

Wallace, J. M., quoted by R. A. Kerr, Sunspot-weather link holding up, *Science*, *242*, 1124, 1988.

Wang, P. K., S. N. Grover, and H. R. Pruppacher, On the effect of electric charges on the scavenging of aerosol particles by clouds and small raindrops, *J. Atmos. Sci.*, *35*, 1735, 1978.

R. A. Heelis and B. A. Tinsley, Center for Space Sciences, University of Texas at Dallas, Box 830688, Mail Stop FO22, Richardson, TX 75083 -0688.

(Received July 9, 1992;
revised March 10, 1993;
accepted March 10, 1993.)